Frequency Responses of a Neural Oscillator

Kiyotoshi Matsuoka

June 7, 2013

Department of Brain Science and Engineering, Kyushu Institute of Technology

Hibikino, Wakamatsu-ku, Kitakyushu, Japan

matsuoka@brain.kyutech.ac.jp

Abstract

The Matsuoka oscillator has been used to control various robots that perform rhythmic movements. The oscillator-driven control system usually takes a feedback structure. While the oscillator actuates some part of a controlled object, some state variable of the object is fed back to the oscillator. An important property of this control scheme is that the oscillator comes to drive the object at its natural frequency, not at the inherent frequency of the oscillator. Although there are some works that intend to elucidate the mechanism of this resonance tuning, they are mostly based on simulations or graphical analyses. It seems therefore difficult to draw a clear, general conclusion from those results. This article expresses the input-output relation of the oscillator in a form of describing function. Based on the function, the unique characteristics of the Matsuoka oscillator and the mechanism of resonance tuning are explained clearly.

central pattern generator, the Matsuoka oscillator, describing function, resonance tuning, entrainment

1 Introduction

The model of central pattern generators proposed by the author [1, 2] has been applied to various robots that perform rhythmic movements, particularly to locomotive robots. The model is composed of two identical, spontaneously firing neurons that are coupled in a symmetric way; one neuron's firing suppresses the other neuron's activity. This reciprocal inhibition between the neurons produces a sustained oscillation.

The oscillator-driven control system usually takes a feedback structure. While the oscillator actuates some part of a controlled object or robot, some state variable of the object is fed back to the oscillator as input. Namely, the oscillator is not used just as a driver, but as an input-output element or controller. The

most important property of this control scheme is that the oscillator adapts to the object dynamics and drives the object at the object's natural frequency, not at the oscillator's inherent frequency.

Although there are some works that intend to clarify the mechanism of the resonance tuning, they are mostly based on simulations or graphical analyses such as the Bode and Nyquist plots [3, 4, 5]. In those works the results are given only to some particular sets of parameter values. It is therefore difficult to draw a general conclusion from the results. In particular, it seems to be impossible to quantitatively state how the emergence of resonance tuning depends on the values of the model parameters. That implies that it is difficult to obtain a design guideline for determining the model parameters when given a controlled object.

In this article the input-output relation of the oscillator will be given in a form of describing function, which is a frequency transfer function depending on the input amplitude. All unique properties of the Matsuoka oscillator as a controller will be explained based on the function. The results can be summarized as:

1. Properties of the oscillator as an input-output system
   (a) When the amplitude A of the sinusoidal input is relatively small, the output of the oscillator becomes a mixture of an oscillator-originated oscillation and an input-originated one. As the input amplitude increases and exceeds a critical value $A_0(\omega)$, where ω is the input frequency, the so-called entrainment occurs; namely, the inherent oscillation originated from the oscillator completely disappears in the output.
   (b) As the the input amplitude increases further, the output amplitude *decreases*; this is a peculiar characteristic of the Matsuoka oscillator used as a controller.
   (c) When the input amplitude reaches a value $A_1(\omega)$, the output totally vanishes.
2. Explicit expressions of the describing function $N(\omega, A)$ in two particular cases
   (a) When the amplitude of the input is close to $A_0(\omega)$ or $A_1(\omega)$, the describing function can be given in explicit forms.
   (b) In respect of the phase characteristic, the oscillator works as a kind of first-order linear system for a large input amplitude, but the gain characteristic is completely different.
3. Properties of an oscillator-driven feedback system
   (a) When the oscillator is coupled with a mass-spring-damper system with a high feedback gain, the oscillation generated is completely different from the inherent oscillation generated by the oscillator alone.

(b) Resonance tuning to the natural frequency ω_p of the controlled object occurs when ω_p is larger than a value ω_1, which is a function of a time constant of the oscillator.

It should be stressed that all these results are given by mathematically explicit expressions; $N(\omega, A)$, $A_0(\omega)$, $A_1(\omega)$ and others will all be given as specific functions of the model parameters.

The approach addressed in this article has some merits. First, it can explain the mechanism of resonance tuning more clearly than simulations or graphical methods. Second, it will give a specific guideline to determine the model parameters in the design of the oscillator-driven control system.

2 The Neural Oscillator

In this section we shall give a brief sketch about the Matsuoka oscillator. An important point is that the frequency and amplitude of the oscillation generated by the oscillator *alone* can be predicted with explicit functions of the model parameters. The theoretically predicted frequency ω_n and amplitude A_n will also appear in the following sections.

2.1 The model

The oscillator model proposed by the author [1, 2] is composed of two identical neurons. The dynamics of each neuron is given by the following second-order system of differential equations, so that the whole system is of fourth order:

$$\tau \frac{d}{dt} x_i(t) + x_i(t) = c - a y_j(t) - b v_i(t) \quad (i, j = 1, 2; i \neq j), \tag{1}$$

$$T \frac{d}{dt} v_i(t) + v_i(t) = y_i(t), \tag{2}$$

$$y_i(t) = g(x_i(t)). \tag{3}$$

Variables $x_i(t)$ and $y_i(t)$ represent the membrane potential and the firing *rate* of neuron i, respectively. Neuron i receives a tonic input $c\ (> 0)$ and an inhibitory input $-a y_j(t)$ from the other neuron $j\ (\neq i)$. Variable $v_i(t)$ represents an adaptation property ubiquitously seen in real neurons, and works as a self-inhibitory input. Note that the model describes a relatively long time-scale behavior of the neurons; variable $y_i(t)$ does not represent the behavior of individual spikes produced by the neuron, but the spike frequency.

Function g is defined as $g(x) \triangleq \max\{0, x\}$; it embodies a threshold characteristic of the neuron's firing. Although g is nonlinear, it has a linearity in a limited sense: $g(\alpha x) = \alpha g(x)$ $(\alpha \geq 0)$. This scaling linearity enables the relatively easy treatment of the present model.

2.2 Condition for stable oscillation

The reciprocal inhibition between the neurons and the adaptation (self inhibition) both play essential roles for rhythm generation. Without either of them the neural circuit cannot produce a stable oscillation. The condition for the stable limit cycle is given by [1] as

$$1 + \frac{\tau}{T} < a < 1 + b. \tag{4}$$

Parameters a (> 0) and b (> 0) represent the strength of reciprocal and self inhibitions; τ (> 0) and T (> 0) are the time constants that determine the reaction times of variables $x_i(t)$ and $v_i(t)$, respectively.

The first inequality in (4) demands that the reciprocal inhibition be strong enough to prevent simultaneous firing of the two neurons. The second inequality requires the adaptation to be sufficiently strong so as to prevent unilateral excitation of either neuron. Throughout this article the model parameters are assumed to satisfy (4).

2.3 Frequency and amplitude of the oscillation

In [1] the author showed the condition for the stable oscillation, but gave no description about how the frequency and amplitude of the oscillation depend on the model parameters. In the literature, a lot of mathematical analyses for various neural oscillators or CPG models can be seen. Some of the mathematical techniques used in them are: the singular perturbation theory [6], a method for piecewise linear systems [7], a method of averaging [8], harmonic balance [9], the phase plane analysis [10]. However, few reports give mathematically explicit relations between the frequency/amplitude of the oscillation and the model parameters. Recently the author obtained explicit expressions for that by means of the describing function analysis (DFA) [11].

According to the analytical result, the (angular) frequency of the oscillation is around

$$\omega_n \triangleq \frac{1}{T}\sqrt{\frac{(\tau + T)\, b}{\tau a} - 1}. \tag{5}$$

This result suggests an interesting parameter setting. If parameters a and b are set equal, then ω_n takes a remarkably simple form as $\omega_n = \frac{1}{\sqrt{\tau T}}$.

The amplitude of the fundamental harmonic component in $x_i(t)$ proves to be around

$$A_n \triangleq \frac{c}{K^{-1}(K_n) + (a + b)\, L\left(K^{-1}(K_n)\right)}, \tag{6}$$

where K_n is defined by

$$K_n \triangleq \frac{\tau + T}{Ta} = \frac{\tau T \omega_n^2 - 1}{b - a}. \tag{7}$$

Because of the first inequality in (4), K_n takes a value between 0 and 1. The definition of functions K and L will be given in the next section. They are very complicated functions, but (6) can well be approximated by a much simpler expression:

$$A_n \approx \frac{c}{2K_n - 1 + \frac{2}{\pi}(a+b)\sin^{-1}(K_n)}. \tag{8}$$

Indices ω_n, A_n, and K_n will appear as important parameters also in the following sections. The reader might have a question of how the above result can be derived, but there is no need to read the article [11]. A quite simple proof will be given based on the result obtained in subsection 4.1.

3 Describing Function of the Oscillator

The objective of this section is to derive the describing function of the oscillator as an input-output system.

3.1 The oscillator as an input-output system

When the oscillator is used to drive an actuator such as an electric motor mounted on a robot, the difference $y(t)$ of outputs $y_1(t)$ and $y_2(t)$ is usually used:

$$y(t) = y_2(t) - y_1(t). \tag{9}$$

The most important feature of the oscillator-driven control system is that the oscillator does not only drive a controlled object or a *plant* in terminology of control theory, but also receives some state variable $u(t)$ from the plant as input. This feedback structure enables the oscillator to adapt to the plant dynamics and perform an energy-efficient driving. Although several input methods are conceivable, most researchers have adopted the following method [3]:

$$\tau\frac{d}{dt}x_i(t) + x_i(t) = c - ay_j(t) - bv_i(t) - g(\pm u(t)). \tag{10}$$

Namely, each neuron receives $-g(\pm u(t))$ as input. Symbol $\pm$ takes $+$ or $-$ for $i = 1$ or $i = 2$, respectively; when $u(t)$ takes a positive / negative value, it gives an inhibitory input to neuron 1 / 2 and zero input to neuron 2 / 1.

An interesting feature of this input method is that, since $y_j(t)$, $v_i(t)$, and $g(\pm u(t))$ are all non-negative, the right-hand side of (10) never exceeds positive constant c, implying that $x_i(t)$ is bounded to the upper by c. This leads to $0 \le y_i(t) \le c$ and hence $-c \le y(t) \le c$. Therefore, if the plant is a bounded-input bounded-output stable system, its output does not diverge unstably even if the feedback gain in the system is set arbitrarily large.

For a summary we here write the whole set of equations of the oscillator as an input-output system:

$$\tau \frac{d}{dt} x_i(t) + x_i(t) = c - a y_j(t) - b v_i(t) - g(\pm u(t)), \tag{11}$$

$$T \frac{d}{dt} v_i(t) + v_i(t) = y_i(t) = g(x_i(t)), \tag{12}$$

$$y(t) = y_2(t) - y_1(t). \tag{13}$$

3.2 DFA of nonlinear element g

The oscillator includes four nonlinear elements, but they are all the same: $g(u) = \max\{0, u\}$. Before calculating the describing function of the whole system, we apply DFA to this (memoriless) nonlinear element.

Let $u(t)$ be an input to g and assume that it is a purely sinusoidal wave with frequency ω, amplitude A, and bias d:

$$u(t) = A\cos(\omega t) + d = A(\cos(\omega t) + r) \quad (A \geq 0), \tag{14}$$

where r is the ratio of the bias to the amplitude, $r = \frac{d}{A}$. Parameter r may take any positive or negative value. Then, the output of g can be written as

$$\begin{aligned} g(u(t)) &= g(A(\cos(\omega t) + r)) = A g(\cos(\omega t) + r) \\ &= A(K(r)\cos(\omega t) + L(r)) \\ &\quad + \text{higher-order harmonics of } \omega. \end{aligned} \tag{15}$$

Note that the scaling linearity of g is essential and that $K(r)$ and $L(r)$ are functions only of r. Function $K(r)$ represents the amplitude ratio between the fundamental harmonic components of the output and the input. Function $L(r)$ is the ratio of the output bias to the input amplitude. Henceforth we neglect higher-order harmonic terms in this kind of equations; eqn (15) is written simply as $g(u(t)) = A(K(r)\cos(\omega t) + L(r))$. It can also be written as

$$g(u(t)) = K(r)\,\widetilde{u}(t) + AL(r). \tag{16}$$

Variable $\widetilde{u}(t)$ denotes the fundamental harmonic component in $u(t)$: $\widetilde{u}(t) = A\cos(\omega t)$ in this case.

Eqn (16) is a linearized equation that represents the input-output relation of g, but actually it is not linear because coefficients $K(r)$ and $AL(r)$ depend on the amplitude and bias of the input. Symbol $\widetilde{\ }$ will also be used for other variables in the same meaning, i.e., fundamental harmonic components in $x_i(t)$, $y_i(t)$ and $v_i(t)$ are denoted as $\widetilde{x}_i(t)$, $\widetilde{y}_i(t)$ and $\widetilde{v}_i(t)$, respectively.

Functions $K(r)$ and $L(r)$ are given by

$$K(r) = \begin{cases} 0 & (r < -1) \\ \frac{1}{\pi}\left(\sqrt{1-r^2}\,r - \cos^{-1}(r)\right) + 1 & (-1 \leq r \leq 1) \\ 1 & (r > 1), \end{cases} \tag{17}$$

$$L(r) = \begin{cases} 0 & (r < -1) \\ \frac{1}{\pi}\left(\sqrt{1-r^2} - r\cos^{-1}(r)\right) + r & (-1 \le r \le 1) \\ r & (r > 1), \end{cases} \tag{18}$$

where $\cos^{-1}(r)$ is defined such that $0 \le \cos^{-1}(r) \le \pi$. The derivation is given in Appendix A. The graphs of the functions for $-1 \le r \le 1$ are shown in Fig.1 (left and middle).

Functions $K(r)$ and $L(r)$ are monotonically increasing functions, and their ranges are $0 \le K(r) \le 1$ and $0 \le L(r) < \infty$. In the DFA the input to g is assumed to be a sinusoidal wave with a bias. Obviously, when $K(r)$ is small, $g(u(t))$ deviates from a pure sinusoid due to the distortion induced by g. For $r \le -1$ or $K(r) = 0$ or $L(r) = 0$, the output vanishes: $g(u(t)) \equiv 0$. Conversely, when $K(r)$ is large, the distortion is small and hence the accuracy of the obtained result will be high. For $r \ge 1$ or $K(r) = 1$ or $L(r) \ge 1$, no distortion is induced by g: $g(u(t)) \equiv u(t)$. Thus, $K(r)$ can be used as an index for evaluating the accuracy or validity of the above analysis. It is easy to find that $K(0) = \frac{1}{2}$ and $L(0) = \frac{1}{\pi}$.

A rough approximation of $K(r)$ is

$$K(r) \approx \frac{r+1}{2} \quad (-1 \le r \le 1), \tag{19}$$

and function $L(r)$ can be approximated *as a function of* $K(r)$ as

$$L(r) \approx \frac{2}{\pi}\sin^{-1}(K(r)) \quad (-1 \le r \le 1), \tag{20}$$

where $\sin^{-1}(K)$ $(0 \le K \le 1)$ is defined such that $0 \le \sin^{-1}(K) \le \frac{\pi}{2}$. Actually, the form $r \approx 2K(r) - 1$ will be used rather than (19). The validity of (20) can be seen in Fig.1 (right), which is a K versus L graph. The thin curve in the figure is a parametric representation of $(K(r), L(r))$ $(-1 \le r \le 1)$ where $K(r)$ and $L(r)$ are given by (17) and (18), and the thick curve represents function $L = \frac{2}{\pi}\sin^{-1}(K)$. It can be seen that the two curves remarkably coincide. The derivation of (8) from (6) was made by using these approximations.

When r is close to ± 1, neither (19) nor (20) however gives good approximations. In section 5 the describing function with $r \approx -1$ will be investigated. More accurate approximations of $K(r)$ and $L(r)$ are required in the case and they are given in Appendix B.

In this subsection, variable $u(t)$ has been assumed to be an input to any of the four nonlinear elements. Henceforth, symbol $u(t)$ will be used solely for the input to the whole oscillator, i.e., the input to g in (11), not in (12). We only consider the case that $u(t)$ has no bias: $u(t) = \widetilde{u}(t) = A\cos(\omega t)$. Then we find that

$$g(\pm u(t)) = A(\pm K(0)\cos(\omega t) + L(0)) = \pm\frac{1}{2}u(t) + \frac{1}{\pi}A. \tag{21}$$

Note that $g(x_i(t))$ cannot be expressed in such a simple form as above because $x_i(t)$ has a nontrivial bias.

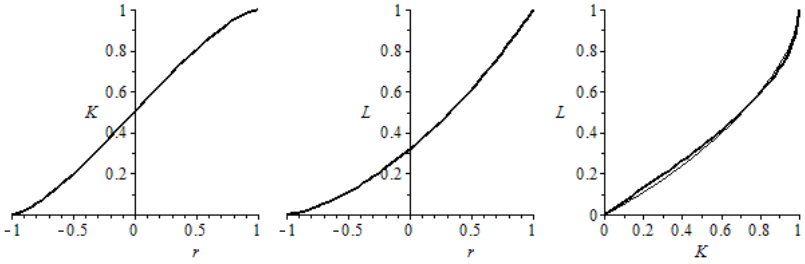

Figure 1: Functions $K(r)$ (left), $L(r)$ (middle), and $L(K)$ (right). In the right figure, the thin curve represents the exact relation between $K(r)$ and $L(r)$ and the thick curve is its approximation given by eqn (20). $L(r)$ of the latter curve takes a slightly larger / smaller value than that of the former curve for a range of small / large K.

3.3 The describing function of the oscillator

In this subsection we assume that the amplitude of the oscillator's input is sufficiently large and the output therefore becomes a purely periodic wave of the input's frequency. Namely, we consider the situation that a perfect entrainment to the input occurs. Let $x_i(t)$ $(i = 1, 2)$ be

$$x_i(t) = A_x(\cos(\omega t + \varphi_i) + r_x) = \widetilde{x}_i(t) + A_x r_x \quad (A_x \geq 0), \tag{22}$$

in which higher-order harmonics are neglected. Parameter r_x is the ratio of the bias to the amplitude of $x_i(t)$. We assume that $x_1(t)$ and $x_2(t)$ behave in a symmetrical manner, i.e., both are expressed by (22) but with $\varphi_1 = \varphi_2 + \pi$. Then we have $\widetilde{x}_2(t) = -\widetilde{x}_1(t)$.

Utilizing (16), we can express variable $y_i(t) = g(x_i(t))$ as

$$y_i(t) \quad = \quad K(r_x)\widetilde{x}_i(t) + A_x L(r_x). \tag{23}$$

Variable $v_i(t)$ can be expressed as

$$v_i(t) = \widetilde{v}_i(t) + A_x L(r_x), \tag{24}$$

because, according to eqn (12), the bias component of $v_i(t)$ is equal to that of $y_i(t)$. Substituting (21), (22), (23) and (24) into (11) and (12) leads to

$$\begin{aligned} \tau\frac{d}{dt}\widetilde{x}_i(t) + \widetilde{x}_i(t) + A_x r_x \quad = \quad & c - a(K(r_x)\tilde{x}_j(t) + A_x L(r_x)) \\ & -b(\tilde{v}_i(t) + A_x L(r_x)) \\ & -\left(\pm\frac{1}{2}u(t) + \frac{1}{\pi}A\right), \end{aligned} \tag{25}$$

$$T\frac{d}{dt}\tilde{v}_i(t) + \tilde{v}_i(t) = K(r_x)\tilde{x}_i(t). \tag{26}$$

Further defining $x(t) \stackrel{\triangle}{=} \widetilde{x}_2(t) - \widetilde{x}_1(t)$ and $v(t) \stackrel{\triangle}{=} \widetilde{v}_2(t) - \widetilde{v}_1(t)$, we have

$$\tau \frac{d}{dt} x(t) + (1 - aK(r_x)) x(t) = -bv(t) + u(t), \tag{27}$$

$$T \frac{d}{dt} v(t) + v(t) = K(r_x) x(t), \tag{28}$$

$$y(t) = K(r_x) x(t). \tag{29}$$

We have now obtained a set of linearized equations that relates input $u(t)$ and output $y(t)$, but note that $K(r_x)$ depends on the frequency ω and amplitude A of $u(t)$. A trivial but important conclusion is that the vanishment of the output occurs if $K(r_x) = 0$.

Applying the Laplace transform to (27) and (28), we obtain the transfer function or describing function from $u(t)$ to $x(t)$:

$$\begin{aligned} G(s, A) &= \frac{1}{\tau s + 1 - K(r_x)\left(a - \frac{b}{Ts+1}\right)} && (30) \\ &= \frac{Ts + 1}{\tau T s^2 + (\tau + T - TaK(r_x)) s + 1 + (b - a) K(r_x)} \\ &= \frac{Ts + 1}{\tau T s^2 + (K_n - K(r_x)) Tas + 1 + (\tau T \omega_n^2 - 1) \frac{K(r_x)}{K_n}}. && (31) \end{aligned}$$

The third equality comes from (7). The constant term in the denominator, $1 + \left(\tau T \omega_n^2 - 1\right) \frac{K(r_x)}{K_n}$ $(= 1 + (b - a) K(r_x))$, is always positive because of the second inequality in (4) and $0 \leq K(r_x) \leq 1$. On the other hand, the coefficient of the s term, $(K_n - K(r_x)) Ta$ $(= \tau + T - TaK(r_x))$, can take a positive as well as negative value. However, it should be noted that the above function has been derived on the assumption that $K_n - K(r_x) > 0$, because otherwise the system becomes unstable.

Precisely speaking, the describing function should be written in a form of frequency transfer function as

$$\begin{aligned} G(\omega, A) &= \frac{1}{j\tau\omega + 1 - K(r_x)\left(a - \frac{b}{jT\omega+1}\right)} && (32) \\ &= \frac{jT\omega + 1}{1 + (\tau T \omega_n^2 - 1) \frac{K(r_x)}{K_n} - \tau T \omega^2 + j (K_n - K(r_x)) Ta\omega}. && (33) \end{aligned}$$

but expressions like (31) will also be used for its clarity. The describing function from $u(t)$ to $y(t)$ is

$$N(\omega, A) = K(r_x) G(\omega, A). \tag{34}$$

Two forms are given to $G(\omega, A)$ because two particular cases are investigated later: $K(r_x) = 0$ and $K(r_x) = K_n$. In the former case, (32) directly leads to $G(\omega, A) = \frac{1}{j\tau\omega+1}$; in the latter case, (33) directly leads to $G(\omega, A) = \frac{jT\omega+1}{\tau T(\omega_n^2-\omega^2)}$.

Because the gain from $u(t)$ to $x(t)$ is $|G(\omega, A)|$, the amplitude of $x(t)$ is given by $|G(\omega, A)|A$. Since $x(t) = \widetilde{x}_2(t) - \widetilde{x}_1(t) = -2\widetilde{x}_1(t) = 2\widetilde{x}_2(t)$, the amplitude A_x of $x_i(t)$ is half that of $x(t)$. Thus we have

$$A_x = \frac{1}{2}|G(\omega, A)|A. \tag{35}$$

3.4 Calculation of r_x

Describing function $G(\omega, A)$ is a very complicated function because r_x is a complicated function with respect of ω and A. $r_x = r_x(\omega, A)$ can be determined in the following way. Extracting the bias components from (25), we have $A_x r_x = c - aA_x L(r_x) - bA_x L(r_x) - \frac{1}{\pi}A$ or

$$A_x\{r_x + (a+b)L(r_x)\} = c - \frac{1}{\pi}A. \tag{36}$$

Combining (35) and (36), we obtain

$$\{r_x + (a+b)L(r_x)\}\,|G(\omega, A)| = 2\left(\frac{c}{A} - \frac{1}{\pi}\right), \tag{37}$$

i.e.,

$$\frac{r_x + (a+b)L(r_x)}{|j\tau\omega + 1 - K(r_x(\omega, A))\left(a - \frac{b}{jT\omega+1}\right)|} = 2\left(\frac{c}{A} - \frac{1}{\pi}\right) \tag{38}$$

or

$$\frac{\{r_x + (a+b)L(r_x)\}\,|jT\omega + 1|}{|1 + (\tau T\omega_n^2 - 1)\,\frac{K(r_x)}{K_n} - \tau T\omega^2 + j\,(K_n - K(r_x))\,Ta\omega|} = 2\left(\frac{c}{A} - \frac{1}{\pi}\right). \tag{39}$$

This equation defines function $r_x = r_x(\omega, A)$, but *implicitly*. We assume that $K(r_x) < K_n$; only this case is significant as described in the last subsection. On this matter a more detailed discussion will be made in subsection 4.1.

Henceforth we assume that the model parameters are set such that $r_x(\omega, A)$ is uniquely determined and it is a decreasing function with respect to A. A typical choice of the model parameters for that is $a = b$ and hence $\omega_n = \frac{1}{\sqrt{\tau T}}$, which was referred to in subsection 2.3. Then, eqn (39) reduces to

$$\frac{(r_x + 2aL(r_x))\,|1 + jT\omega|}{|1 - \left(\frac{\omega}{\omega_n}\right)^2 + j\,(K_n - K(r_x))\,Ta\omega|} = 2\left(\frac{c}{A} - \frac{1}{\pi}\right). \tag{40}$$

Then, the left-hand side of (40) proves to a strictly increasing function with respect to r_x, while the right-hand side is a strictly decreasing function with

respect to A. Thus, r_x must be uniquely determined for given A, and it must be a decreasing function of A. Since $K(r_x)$ is an increasing function of r_x, it is also a decreasing function of A. In the case of $a \neq b$, however, we have no general theory about the the shape of $r_x(\omega, A)$ at present.

Now we have obtained the complete set of equations that specifies the describing function. Here we write them for a summary:

$$G(\omega, A) = \frac{jT\omega + 1}{1 + (\tau T\omega_n^2 - 1)\frac{K(r_x)}{K_n} - \tau T\omega^2 + j(K_n - K(r_x))Ta\omega}, \quad (41)$$

$$N(\omega, A) = K(r_x)\, G(\omega, A), \quad (42)$$

where r_x is given (implicitly) by

$$\{r_x + (a+b)L(r_x)\}\,|G(\omega, A)| = 2\left(\frac{c}{A} - \frac{1}{\pi}\right). \quad (43)$$

4 Two Critical Amplitudes of the Input

If the amplitude of the sinusoidal input is small, the output will be a mixture of an oscillator-originated wave and an input-originated one. As the amplitude increases and exceeds a critical value, the so-called entrainment occurs; the inherent oscillation originated from the oscillator completely disappears. As the input amplitude increases further and reaches another critical value, the output totally vanishes. In this section we shall find these critical amplitudes. In the analyses, *there is no need to solve (43) with respect to* r_x. The value of $K(r_x)$ (and hence r_x and $L(r_x)$) is first determined from some consideration without (43), and then the critical amplitude is found by solving (43) with respect to A.

4.1 Minimum amplitude for entrainment to the input

Describing function $G(s, A)$ was derived based on the assumption that the oscillator entrains to the sinusoidal input. However, when the input amplitude is too small and hence $K(r_x)$ is large, $G(s, A)$ enters an unstable region. The critical amplitude below which the system becomes unstable can be considered the lower bound of the entrainment.

From (31), the stable-unstable transition is found to occur when

$$K(r_x) = K_n \left(= \frac{\tau + T}{Ta}\right). \quad (44)$$

In this situation, eqn (39) becomes

$$N(s, A) = \frac{K_n(Ts + 1)}{\tau T(s^2 + \omega_n^2)}. \quad (45)$$

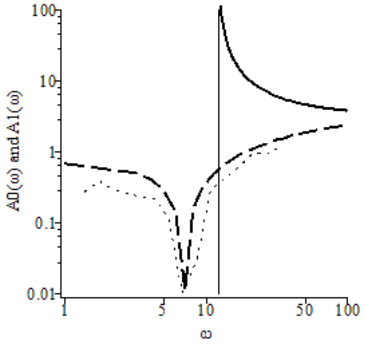

Figure 2: The minimum amplitude $A_0(\omega)$ for entrainment (dashed curve) and the minimum amplitude $A_1(\omega)$ for a vanishing output (solid curve). The dotted line is an experimental result corresponding to $A_0(\omega)$, which is a rough copy from [3]. The vertical line indicates the critical frequency $\omega_1 = 12.1$. $A_0(\omega)$ and $A_1(\omega)$ both converge to $\pi c = 3.14$ for $\omega \to \infty$.

The linear system theory tell us that, without input, this system generates a periodic oscillation of frequency ω_n, which is the inherent frequency of the oscillator. Thus, it can be predicted that the complete entrainment occurs when $K(r_x) < K_n$.

Substituting $K(r_x) = K_n$ into (39) and solving it with respect to A, we find the minimum amplitude of the input for entrainment. We denote it by $A_0(\omega)$:

$$A_0(\omega) = \frac{c}{\frac{1}{2}\frac{\sqrt{T^2\omega^2+1}}{\tau T|\omega^2-\omega_n^2|}\frac{c}{A_n} + \frac{1}{\pi}}. \tag{46}$$

Although A_n is a complicated function of K_n, it can well be approximately by (8). It is easy to find that $A_0(\omega_n) = 0$.

In Fig.2 the graph of $A_0(\omega)$ is illustrated by a dashed line. The model parameters are set as $\tau = 0.1$, $T = 0.2$, $a = b = 2.5$, $c = 1.0$. In this parameter setting, ω_n is 7.1; ω_n is the bottom frequency of the curve. The thin dotted line in the figure shows the corresponding result obtained by a simulation [3]. A remarkable correspondence can be seen between the two curves.

Incidentally, in section 2 the reader might have had a question of how the frequency and amplitude produced by the oscillator without input prove to be ω_n and A_n. Now that we have obtained the above result, the proof is quite simple. The fact that $A_0(\omega_n) = 0$ implies that an oscillation of frequency ω_n emerges without input. Substituting $A = 0$ and $r_x = K^{-1}(K_n)$ into (36) leads to $A_x = \frac{c}{K^{-1}(K_n)+(a+b)L(K^{-1}(K_n))} = A_n$.

4.2 Minimum amplitude of the vanishment of the output

As described in subsection 3.4, the output amplitude of the oscillator decreases with the increase of the input amplitude. When the input amplitude becomes sufficiently large, the output may totally vanish. We can prove that the minimum amplitude for that is

$$A_1(\omega) = \frac{c}{\frac{1}{\pi} - \frac{1}{2}\frac{1}{\sqrt{\tau^2\omega^2+1}}} \ (\omega > \omega_1), \tag{47}$$

where

$$\omega_1 = \frac{\sqrt{\frac{\pi^2}{4} - 1}}{\tau}. \tag{48}$$

This proposition can be proved as follows. When the output is zero, relation $K(r_x) = 0$ holds. That implies $r_x \leq -1$ and hence $L(r_x) = 0$. In this state, eqn (38) reduces to

$$\frac{1}{2}\frac{r_x}{|j\tau\omega + 1|} = \frac{c}{A} - \frac{1}{\pi}. \tag{49}$$

From this and $r_x \leq -1$, we find that, if

$$A \geq \frac{c}{\frac{1}{\pi} - \frac{1}{2}\frac{1}{|j\tau\omega+1|}} = A_1(\omega), \tag{50}$$

then the output vanishes. This result is however valid only in the case of $\frac{1}{\pi} - \frac{1}{2}\frac{1}{|j\tau\omega+1|} > 0$ or $\omega > \omega_1$. The graph of $A_1(\omega)$ $(\omega > \omega_1)$ is shown in Fig.1 (solid curve). The vertical line indicates ω_1.

In the case of $\omega < \omega_1$, the situation becomes completely different. When $A \to \infty$, eqn (43) reads

$$\{r_x + (a+b)L(r_x)\}\,|G(\omega, A)\,| = -\frac{2}{\pi} \tag{51}$$

This equation proves to hold for a value of r_x larger than -1, as follows. For $r_x = -1$ the left-hand side of the above equation takes $-\frac{1}{\sqrt{\tau^2\omega^2+1}}$, which is smaller than the right-hand side, $-\frac{2}{\pi}$, in the case of $\omega < \omega_1$. Since the left-hand side is an increasing function of r_x, the above equation must hold for a value of r_x larger than -1. We thus find that $K(r_x)$ takes a positive (nonzero) value and hence the output never vanishes even if the input amplitude is arbitrarily large, including the limit case of $A \to \infty$.

The fact that the output amplitude of the oscillator decreases with the increase of the input amplitude (and moreover for a high-frequency range the output finally vanishes) reveals a strange characteristic of the Matsuoka oscillator. The peculiarity will be realized if comparing it with the characteristic of a simple saturator: $y(t) = u(t)$ for $|u(t)| < u_0$ and $= u_0$ otherwise. In this case, the output amplitude monotonically increases with the input amplitude

and finally becomes constant. That implies that the gain of the saturator is proportional to $\frac{1}{A}$ for large A. The result obtained in this subsection implies that the gain of the Matsuoka oscillator decreases more sharply than $\frac{1}{A}$. This peculiar characteristic is due to the fact that input $u(t)$ is applied to the neurons in an inhibitory way.

4.3 $A_0(\omega)$ versus $A_1(\omega)$

We have thus found that the describing function obtained is characterized by two functions: $A_0(\omega)$ and $A_1(\omega)$. Function $A_0(\omega)$ characterizes the property of $G(\omega, A)$ for a small amplitude input, while $A_1(\omega)$ characterize that for a large amplitude input. Relation $A_0(\omega) < A_1(\omega)$ holds, and $A_0(\omega)$ and $A_1(\omega)$ both converge to πc in the limit of $\omega \to \infty$. Functions $A_0(\omega)$ and $A_1(\omega)$ are characterized by critical frequencies ω_n and ω_1, respectively.

An interesting finding is that $A_1(\omega)$ does not depends on a, b, or T, but only on τ and c. That contrasts $A_0(\omega)$, which depends on all the model parameters.

When the oscillator is used as a controller, the amplitude A of the input should be between $A_0(\omega)$ and $A_1(\omega)$. In the oscillator-driven control system, frequency ω_1 is more important than ω_n because the feedback gain is usually set to be high and hence the amplitude of the oscillator's input is large.

4.4 Examples

Here we show two simulations. In both, the parameters of the oscillator are set as $a = 2.5$, $b = 2.5$, $c = 1.0$, $\tau = 0.1$, $T = 0.2$. The inherent frequency ω_n calculated by (5) is 7.1; the critical frequency ω_1 calculated by (48) is 12.1.

In the first simulation the frequency of the input is fixed at $\omega = 50$, which is larger than ω_1. Fig.3 shows the output of the oscillator for several amplitudes of the input. It can be seen that entrainment occurs at amplitudes larger than around 1.6; the theoretically estimated amplitude for that is $A_0(50) = 1.82$. As the amplitude increases further and reaches around $A = 4.6$, the output vanishes completely; the theoretical prediction is $A_1(50) = 4.54$.

In the second simulation, the input frequency is set at $\omega = 4$, which is smaller than ω_1. It can be seen that entrainment occurs around $A = 0.3$; the corresponding theoretical prediction is $A_0(4) = 0.41$. The output vanishes at a very large value of A, around 8000. The theoretical analysis however predicts that the output never vanishes at $\omega < \omega_1$. This discrepancy is due to inaccuracy of the DFA for low-frequency input; this matter will be discussed in the next subsection. In spite of such a discrepancy, the argument in subsection 4.2 well explains why the frequency response of the oscillator for large input differs radically between the low and high frequency ranges.

4.5 On accuracy of DFA

It should be noted that the DFA, in which all higher-order harmonic components are neglected, is a rough approximation method. Here we give some comments

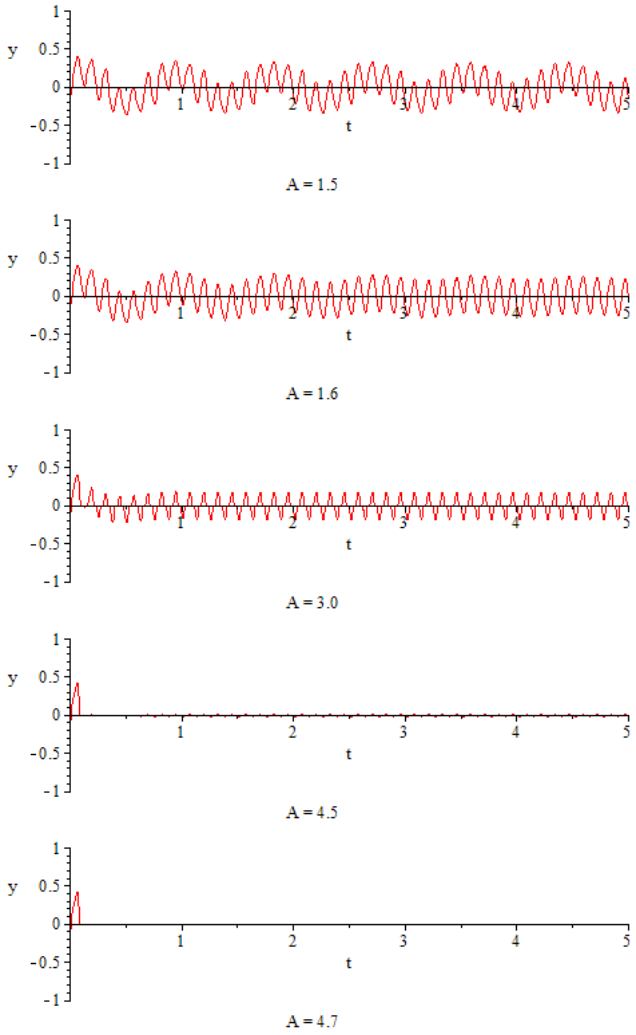

Figure 3: The output of the oscillator with variable amplitude A and fixed frequency $\omega = 50$ of the input.

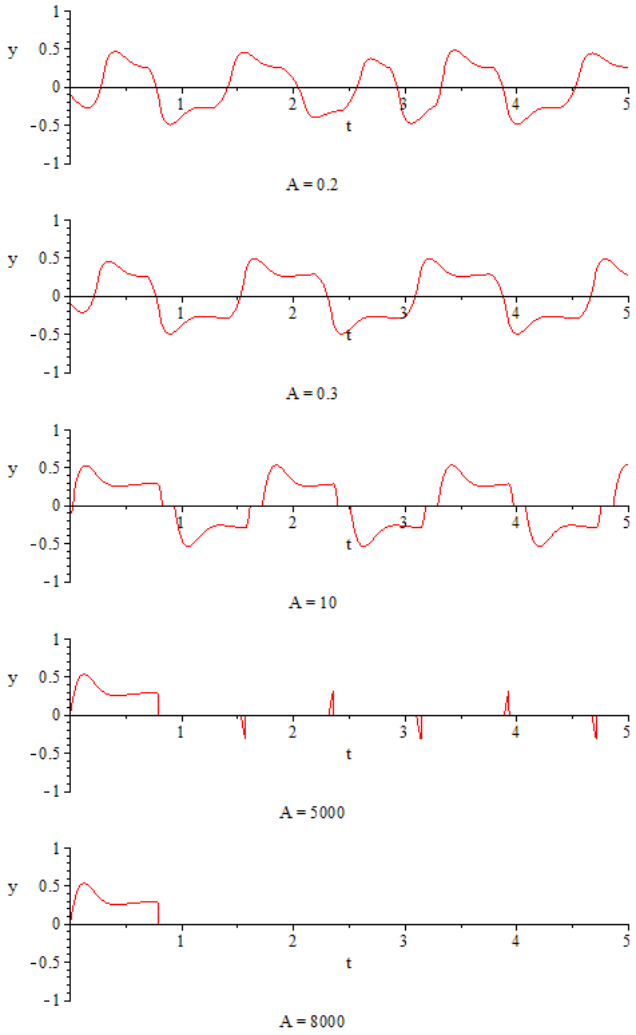

Figure 4: The output of the oscillator with variable amplitude A and fixed frequency $\omega = 4$ of the input.

on inaccuracy associated with the method. The inaccuracy becomes serious particularly in two cases.

One is the case that the frequency of the input to the oscillator is very low. The DFA assumes that higher order harmonics rapidly decay through some low-pass filtering elements in the system. Therefore, if the method is applied to a low-frequency range (more specifically, if $\omega \ll \frac{1}{\tau}, \frac{1}{T}$), it does not give a good approximation. For example, let us consider an extreme parameter setting: $a = b = c = 0$. In this case, for a very low frequency range, eqn (11) reduces to a static equation $x_i(t) = -g(\pm u(t)) \leq 0$ and hence $y(t) = g(x_2(t)) - g(x_1(t)) = 0$; i.e., the output vanishes. The DFA however yields a different result. From eqn (21), we have

$$x_i(t) = -g(\pm A\cos(\omega t)) = \frac{A}{2}\left(\mp\cos(\omega t) - \frac{2}{\pi}\right) \tag{52}$$

and hence

$$y_i(t) = g(x_i(t)) = \frac{A}{2}\left(\mp K\left(-\frac{2}{\pi}\right)\cos(\omega t) + L\left(-\frac{2}{\pi}\right)\right) \tag{53}$$

and

$$\begin{aligned} y(t) &= y_2(t) - y_1(t) \\ &= AK\left(-\frac{2}{\pi}\right)\cos(\omega t) = K\left(-\frac{2}{\pi}\right)u(t) \approx 0.12u(t). \end{aligned} \tag{54}$$

Thus the oscillator appears to produce a nonzero output, but that is not the reality. The DFA does not give a good approximation for a low frequency range.

Another problematic case occurs when the amplitude of the input to the oscillator is close to $A_1(\omega)$. As the amplitude A increases, r_x decreases and hence $K(r_x)$ becomes small. The smallness of $K(r_x)$ implies that distortion induced by the nonlinear operation $g(x_i(t))$ is large, which will lower the accuracy of the DFA.

In spite of these problems, the DFA provides considerably accurate predictions for the quantitative characteristics of the oscillator, as has been seen in this section and as will be seen in section 6.

5 Describing Function in Two Particular Cases

In section 3 we derived the describing function of the oscillator, but $K(r_x)$ in it was not expressed as an explicit function of ω and A. In this section we consider the case that A is close to $A_0(\omega)$ or $A_1(\omega)$ (but satisfies $A_0(\omega) < A < A_1(\omega)$). In these cases the describing function can be given in explicit forms.

5.1 The case of $A \approx A_1(\omega)$ $(\omega > \omega_1)$

In this case, $K(r_x)$ becomes very small, and hence the transfer function reduces to

$$N(s, A) \approx \frac{K(r_x)}{\tau s + 1}. \tag{55}$$

In order to express $K(r_x)$ in an explicit form, it will be required to *express* r_x *and* $L(r_x)$ *as functions of* $K(r_x)$. In subsection 3.2 an idea for approximation was shown ((19) and (20)), but they are not sufficiently accurate for $r_x \approx -1$. More accurate approximations in the case are given in Appendix B. They are

$$r_x \approx \frac{1}{2}\left(\frac{3\pi}{2}\right)^{\frac{2}{3}} K(r_x)^{\frac{2}{3}} - 1, \tag{56}$$

$$L(r_x) \approx \frac{1}{2} K(r_x). \tag{57}$$

Eqn (38) can thus be approximated as

$$\frac{\frac{1}{2}\left(\frac{3\pi}{2}\right)^{\frac{2}{3}} K(r_x)^{\frac{2}{3}} - 1 + \frac{1}{2}(a+b)K(r_x)}{|j\tau\omega + 1 - K(r_x)\left(a - \frac{b}{jT\omega+1}\right)|} \approx 2\left(\frac{c}{A} - \frac{1}{\pi}\right). \tag{58}$$

For $K(r_x) \ll 1$, relation $K(r_x)^{\frac{2}{3}} \gg K(r_x)$ holds, leading to

$$\frac{\frac{1}{2}\left(\frac{3\pi}{2}\right)^{\frac{2}{3}} K(r_x)^{\frac{2}{3}} - 1}{\sqrt{\tau^2\omega^2 + 1}} \approx 2\left(\frac{c}{A} - \frac{1}{\pi}\right) \tag{59}$$

and hence

$$K(r_x) \approx \frac{4\sqrt{2}}{3\pi}\left\{1 - 2\left(\frac{1}{\pi} - \frac{c}{A}\right)\sqrt{\tau^2\omega^2 + 1}\right\}^{\frac{3}{2}}. \tag{60}$$

Thus, we obtain the describing function in an explicit form:

$$N(\omega, A) \approx \frac{4\sqrt{2}}{3\pi} \frac{\left\{1 - 2\left(\frac{1}{\pi} - \frac{c}{A}\right)\sqrt{\tau^2\omega^2 + 1}\right\}^{\frac{3}{2}}}{j\tau\omega + 1}. \tag{61}$$

As ω increases with fixed A $(> \pi c)$, the gain $|N(\omega, A)|$ decreases monotonically, and when ω reaches $A_1^{-1}(A) = \frac{\sqrt{\frac{1}{4\left(\frac{1}{\pi} - \frac{c}{A}\right)^2} - 1}}{\tau}$, the value of $|N(\omega, A)|$ becomes zero. With respect to the phase characteristic, the oscillator behaves as a first-order linear system $\frac{const.}{j\tau\omega+1}$, but its gain characteristic is completely different. The gain of the oscillator decreases much more sharply than that of the linear system.

5.2 The case of $A \approx A_0(\omega)$

In this case, we have $K(r_x) \approx K_n$ ($K(r_x) < K_n$) and hence

$$N(s, A) \approx \frac{K_n (Ts + 1)}{\tau T \{s^2 + (K_n - K(r_x))Tas + \omega_n^2\}}. \tag{62}$$

Obviously this is very different from (55). The phase drastically change around $\omega = \omega_n$. For $\omega < \omega_n$, $\angle N(\omega, A) \approx \tan^{-1}(T\omega)$, while for $\omega > \omega_n$, $\angle N(\omega, A) \approx \tan^{-1}(T\omega) - \pi$. The gain $|N(\omega, A)|$ has a sharp peak at around ω_n; that contrasts the gain characteristic of (61), the gain of which is a monotonically decreasing function of ω.

6 Feedback System with a Neural Oscillator

This section considers a feedback system; the output of the oscillator is used to drive a linear system *with a high feedback gain*, while the output of the plant is fed back to the oscillator as input. The result in the last section suggests that the oscillator should not be used with a low feedback gain. In this case the input amplitude becomes small and hence the oscillator works as (62). Then, the characteristic of the overall system will be strongly affected by ω_n and resonance tuning to the natural frequency of the plant will become difficult.

6.1 Feedback system

Let the transfer function of the plant be $P(s)$. Then, the system equations are

$$Y(s) = N(s, A)U(s), \tag{63}$$

$$U(s) = -P(s)HY(s), \tag{64}$$

where $U(s)$ and $Y(s)$ are the Laplace transforms of $u(t)$ and $y(t)$, respectively. We investigate the oscillation emerging from the coupled system.

For the plant we consider a second-order linear oscillatory system (a mass-spring-damper system):

$$P(s) = \frac{\omega_p^2}{s^2 + 2\zeta\omega_p s + \omega_p^2}, \tag{65}$$

where parameters ω_p and ζ represent the natural frequency and the damping ratio of the system, respectively.

6.2 Harmonic balance condition

Here we consider the case that the feedback gain H is sufficiently high. In this case the input to the oscillator becomes large and hence $K(r_x)$ becomes very small. Then, the describing function (34) of the oscillator can be approximated by (55).

When a periodic oscillation is sustained, the so-called harmonic balance condition must be satisfied. The condition is $P(j\omega)HN(\omega, A) = -1$ or

$$\frac{\omega_p^2 HK(r_x)}{(\omega_p^2 - \omega^2 + 2j\zeta\omega_p\omega)(j\tau\omega + 1)} = -1. \tag{66}$$

Evidently, the denominator of the left-hand side must be a real number. This gives the frequency ω_r of the limit cycle generated by the feedback system:

$$\omega_r = \omega_p\sqrt{1 + \frac{2\zeta}{\tau\omega_p}}. \tag{67}$$

We refer to this as resonance frequency. If time constant τ is set to be much larger than $\frac{2\zeta}{\omega_p}$, then the resonance frequency will be close to the natural frequency ω_p of the plant.

Substituting $\omega = \omega_p\sqrt{1 + \frac{2\zeta}{\tau\omega_p}}$ into (66), we obtain

$$K(r_x) = \frac{2\zeta}{H}\left(\tau\omega_p + \frac{1}{\tau\omega_p} + 2\right). \tag{68}$$

Using (59), we obtain the amplitude of the input to the oscillator in this situation. Let it be A_r:

$$A_r = \frac{c}{\frac{1}{\pi} + \frac{\frac{1}{2}\left(\frac{3\pi}{2}\right)^{\frac{2}{3}} K(r_x)^{\frac{2}{3}} - 1}{2\sqrt{\tau^2\omega_r^2 + 1}}} = \frac{c}{\frac{1}{\pi} + \frac{\frac{1}{2}\left\{3\pi\frac{\zeta}{H}\left(\tau\omega_p + \frac{1}{\tau\omega_p} + 2\right)\right\}^{\frac{2}{3}} - 1}{2\sqrt{\tau^2\omega_p^2 + 2\zeta\tau\omega_p + 1}}}. \tag{69}$$

An even rougher approximation can be obtained by considering $H \to \infty$:

$$A_r \approx \frac{c}{\frac{1}{\pi} - \frac{1}{2\sqrt{\tau^2\omega_p^2 + 2\zeta\tau\omega_p + 1}}}. \tag{70}$$

Since the amplitude must be positive, the denominator must be positive. This leads to $\omega_p > \frac{\sqrt{\frac{\pi^2}{4} - 1 + \zeta} - \zeta}{\tau}$, but it is automatically satisfied when $\omega_p > \omega_1$.

The key point of the above discussion is that, if feedback gain H and time constant τ are sufficiently large (i.e., ω_1 is sufficiently small compared to ω_p), then the oscillator works as a first-order time lag element and hence produces a phase lag of around $\frac{\pi}{2}$. Therefore, if a mass-spring-damper system, which provides a phase lag of $\frac{\pi}{2}$ at the natural frequency, is coupled with the oscillator, resonance tuning occurs. There is an argument in which the resonance tuning is explained in connection with ω_n [3], but the author's opinion is different. The fact is that the tuning occurs when $\omega_p > \omega_1$; $\omega_1 = \frac{\sqrt{\frac{\pi^2}{4} - 1}}{\tau}$ is unrelated to $\omega_n = \frac{1}{T}\sqrt{\frac{(\tau+T)b}{\tau a} - 1} = \frac{1}{\sqrt{\tau T}}$ (when $a = b$).

Eqn (70) (as well as (67)) does not include the feedback gain H, suggesting that the amplitude of the plant output (or equivalently the oscillator input)

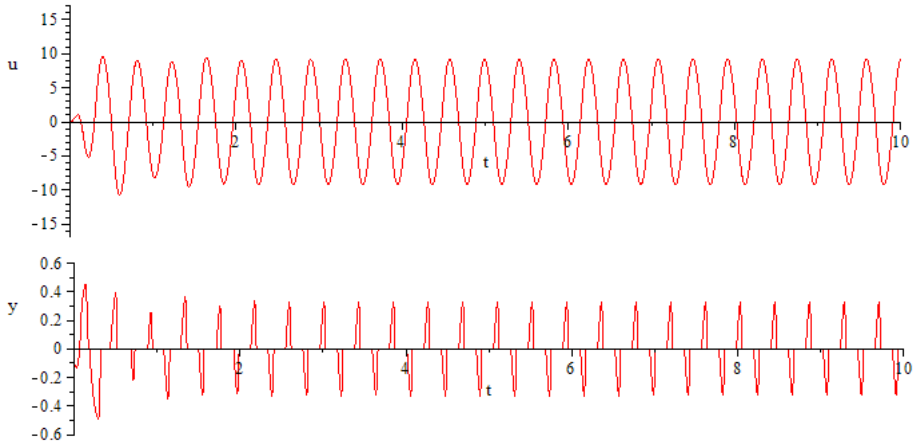

Figure 5: Input $u(t)$ and output $y(t)$ of the oscillator in the feedback system. The natural frequency ω_p of the plant is 15.

is not so sensitive to H if H is large. It is known that the feedback system incorporating the Matsuoka oscillator is very robust. Ferris et al. [12] compared a single pendulum driven by the Matsuoka oscillator and by the van der Pol oscillator, and found that the Matsuoka oscillator entrained the pendulum over a much greater range of feedback gains than the van der Pol oscillator. This robustness is probably related to the fact that the amplitude of the plant output is not so sensitive to the magnitude of H.

6.3 An example

Here we show two examples. The parameters of the oscillator are all the same as those in subsection 4.4. The damping ratio of the plant is set as $\zeta = 0.1$; the feedback gain is $H = 15$; eqn (48) gives $\omega_1 = 12.1$.

In the first example, the natural frequency ω_p of the plant is 15.0, which is larger than ω_1. The simulation result (Fig.5) shows that the frequency of the oscillation generated by the feedback systems is around 15.1, being very close to ω_p. The amplitude is 9.2; the theoretical amplitude A_r calculated by (69) is 9.3. In subsection 3.8, it is pointed out that the DFA becomes inaccurate when the input is large. In spite of that, the theoretically obtained amplitude predicts the actual amplitude with a remarkable accuracy.

Next we look at the case of $\omega_p = 5.0$, which is smaller than ω_1 (Fig.6). The frequency of $u(t)$ is around 5.8. Compared to the case of $\omega_p = 15.0$, its adaptability to the natural frequency of the plant looks low. The theoretical result in the last subsection was derived only for the case of $\omega_p > \omega_1$; for the case of $\omega_p < \omega_1$, we have no theory at present.

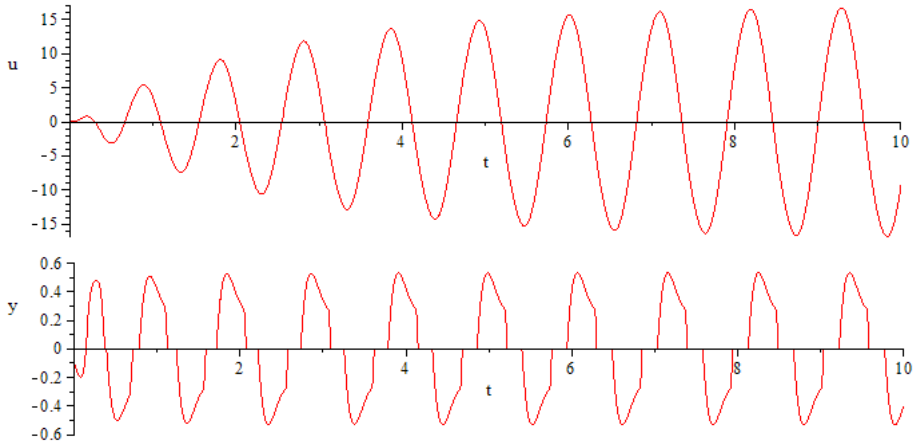

Figure 6: Input $u(t)$ and output $y(t)$ of the oscillator in the feedback system. The natural frequency ω_p of the plant is 5.

7 Concluding Remarks

In this article we have investigated the characteristics of the Matsuoka oscillator as a control element.

First we derived the describing function of the oscillator. Based on it, we derived the lowest amplitude for input entrainment, $A_0(\omega)$, and the lowest amplitude for a vanishing output, $A_1(\omega)$. We also found an important frequency ω_1 that characterizes a peculiar property of the oscillator; it is different from the inherent frequency ω_n of the oscillator. Frequency ω_n determines a critical point in $A_0(\omega)$ while ω_1 gives a critical point in $A_1(\omega)$. Next, we derived explicit expressions of the describing function for two particular cases. Finally we discussed the behavior of a feedback system in which the oscillator is coupled with a mechanical system with a high feedback gain. We analytically derived the resonance frequency ω_r and amplitude A_r.

It should be stressed that, considering that the DFA is a very rough approximation method, the theoretical predictions coincide with the simulation results with remarkable accuracy. The mathematically explicit expressions presented in this article will be helpful in designing oscillator-controlled robots.

References

[1] Kiyotoshi Matsuoka, "Sustained Oscillations Generated by Mutually Inhibiting Neurons with Adaptation," Biological Cybernetics, vol. 52, pp. 367-376, 1985.

[2] Kiyotoshi Matsuoka, "Mechanisms of Frequency and Pattern Control in the Neural Rhythm Generators," Biological Cybernetics, vol. 56, pp. 345-353, 1987.

[3] Matthew M. Williamson, "Neural control of rhythmic arm movements," Neural Networks, vol. 11, pp. 1379-1394, 1998.

[4] T. Iwasaki and M. Zheng, "Sensory feedback mechanism underlying entrainment of central pattern generator to mechanical resonance," Biological Cybernetics, vol. 94, pp. 245-261, 2006.

[5] B. W. Verdaasdonk, H.F.J.M. Koopman, and F.C.T. Van der Helm, "Energy efficient and robust rhythmic limb movement by central pattern generator," Neural Networks, vol. 19, pp. 388-400, 2006.

[6] Adam L. Taylor, Garrison W. Cottrell, and Jr., Williams B. Kristan, "Analysis of oscillations in a reciprocally inhibitory network with synaptic depression," Neural Computation, vol. 14, pp. 561-581, 2002.

[7] Jorge M. Goncalves, "Regions of stability for limit cycles of piecewise linear systems," in IEEE Conference on Decision and Control, 2003.

[8] Daibing Zhang, Dewen Hu, Lincheng Shen, and Haibin Xie, "Dynamical analysis of a novel artificial neural oscillator," Proceedings of the in the 4th International Symposium on Neural Networks, pp. 1061-1068, 2007.

[9] Tetsuya Iwasaki, "Multivariate harmonic balance for central pattern generators," Automatica, vol. 44, pp. 3061-3069, 2008.

[10] Silvia Daun, Jonathan E. Rubin, and Ilya A. Rybak, "Control of oscillation periods and phase durations in half-center central pattern generators: a comparative mechanistic analysis," Journal of Computational Neuroscience, vol. 27, pp. 3-36, 2009.

[11] Kiyotoshi Matsuoka, "Analysis of a Neural Oscillator," Biological Cybernetics, in print.

[12] Daniel P. Ferris, Tiffany L. Viant, and Ryan J. Campbell, “Artificial neural oscillators as controllers for locomotive simulations and robotic exoskeletons,” in 4th World Congress of Biomechanics, 2002.

Appendices

Appendix A: Calculation of $K(r)$ and $L(r)$

Without loss of generality, frequency ω in $\cos(\omega t) + r$ can be assumed to be 1. The interval where $\cos(t) + r$ $(-1 \leq r \leq 1)$ takes a non-negative value in period $[-\pi, \pi]$ is $[-\cos^{-1}(-r), \cos^{-1}(-r)]$. Hence, $K(r)$ and $L(r)$ are calculated as

$$\begin{aligned} K(r) &= \frac{1}{\pi}\int_{-\pi}^{\pi} g(\cos(t)+r)\cos(t)dt \\ &= \frac{1}{\pi}\int_{-\cos^{-1}(-r)}^{\cos^{-1}(-r)} (\cos(t)+r)\cos(t)dt \\ &= \frac{1}{\pi}\left(\sqrt{1-r^2}r - \cos^{-1}(r)\right) + 1, \end{aligned}$$

$$\begin{aligned} L(r) &= \frac{1}{2\pi}\int_{-\pi}^{\pi} g(\cos(t)+r)dt \\ &= \frac{1}{2\pi}\int_{-\cos^{-1}(-r)}^{\cos^{-1}(-r)} (\cos(t)+r)dt \\ &= \frac{1}{\pi}\left(\sqrt{1-r^2} - r\cos^{-1}(r)\right) + r. \end{aligned}$$

The case of $|r| > 1$ is trivial.

Appendix B: Approximation of $K(r)$ and $L(r)$ in the vicinity of $r = -1$

Functions $K(r)$ and $L(r)$ can be expanded in the vicinity of $r = -1$ as

$$K(r) = \frac{4\sqrt{2}}{3\pi}(r+1)^{\frac{3}{2}} - \frac{\sqrt{2}}{5\pi}(r+1)^{\frac{5}{2}} + \cdots,$$

$$L(r) = \frac{2\sqrt{2}}{3\pi}(r+1)^{\frac{3}{2}} + \frac{\sqrt{2}}{30\pi}(r+1)^{\frac{5}{2}} + \cdots.$$

Therefore, r and $L(r)$ can be expressed as as functions of $K(r)$, as

$$r \approx \left(\frac{3\pi}{4\sqrt{2}}K(r)\right)^{\frac{2}{3}} - 1 = \frac{1}{2}\left(\frac{3\pi}{2}\right)^{\frac{2}{3}} K(r)^{\frac{2}{3}} - 1,$$

$$L(r) \approx \frac{1}{2}K(r).$$